ELSEVIER

Journal of Photochemistry and Photobiology A: Chemistry 94 (1996) 89–92

Journal of PHOTOCHEMISTRY AND PHOTOBIOLOGY A:CHEMISTRY

UV multiphoton decomposition of di-*n*-butyl tin diacetate: fluorescence detection of CH radicals

Valerian C. Simianu, Hetvin Andrew Wilkinson, Jeanne M. Hossenlopp *

Marquette University, Department od Chemistry, P.O. Box 1881, Milwaukee, WI 53201-1881, USA

Received 15 August 1995; accepted 20 September 1995

Abstract

Multiphoton-induced fragmentation of di-*n*-butyl tin diacetate was investigated using fluorescence spectroscopy. One-color multiphoton dissociation/laser-induced fluorescence (MPD/LIF) experiments were performed at 236.28 nm and 227.5 nm on gas-phase samples of di-*n*-butyl tin diacetate. These wavelengths correspond to one-photon excitation above the predicted onset of absorption for the dissociative ligand-centered $^1(n,\pi^*)$ transition. With the excitation laser focused into a gas-phase sample, two bands were observed in the dispersed fluorescence spectrum. The band centered at 390 nm was assigned to the CH ($B^2\Sigma$–$X^2\Pi$) 0–0 transition and the band at 430 nm was assigned to the CH ($A^2\Delta$–$X^2\Pi$) transition. Emission from the CH ($B^2\Sigma$–$X^2\Pi$) 1–1 transition was also observed in the MPD/LIF spectrum obtained using 227.5 nm excitation.

Keywords: Multiphoton dissociation; Fluorescence; CH radicals; Photofragment detection

1. Introduction

Comparison of the UV and visible multiphoton dissociation (MPD) patterns of inorganic and organic compounds has been the subject of a great deal of interest. Organometallic compounds have long been known to yield bare metal atoms in resonance-enhanced multiphoton ionization (REMPI) spectroscopic studies. This characteristic pattern of dissociation, followed by ionization, has been termed class B nonlinear photochemistry [1]. Metal atoms are readily detected in the total ion current spectrum, via mass spectrometry or fluorescence. Fragmentation of organic species is known to be dependent on the details of the excitation scheme [1,2], with ionization of the parent compound via intermediate Rydberg states commonly observed.

Di-*n*-butyl tin diacetate (DBTDA) is an example of a compound which may combine features of inorganic and organic MPI patterns. Previous work in our laboratory explored some of the potential one- and multiphoton fragmentation channels of DBTDA [3]. The excitation scheme was based on the use of the ligand-centered $^1(n,\pi^*)$ transition as a dissociative first step in the decomposition. One-photon excitation led to a small amount of CO_2 formation, with an upper limit on the total absolute quantum yield of 2.0×10^{-3}. As expected [1] for a tetravalent tin complex, Sn atomic resonances were observed in the MPI spectrum. In addition, a series of broad features were observed which could not be unambiguously identified via the total ion yield spectrum. In the work reported here, fluorescence spectroscopy is utilized as a complementary technique for the identification of photofragments obtained from DBTDA.

Fluorescence spectroscopy has been shown to be a valuable tool for examining the photofragments produced in MPD experiments and has been applied to organometallic systems. One approach is to monitor the vacuum UV emission produced via electron impact excitation of buffer gases in bulk gas experiments with parallel plate electrodes. This technique provides an alternative detection scheme for MPI spectra and has been applied to arene chromium tricarbonyl compounds [4]. Laser-induced fluorescence (LIF) can be used to monitor the populations of atomic or molecular electronic states which may not be accessible in REMPI experiments due to selection rules. LIF monitoring of metal atoms produced from the MPD of a variety of organometallics and metal alkyl complexes is one example of this type of experiment [5–9]. Fluorescence from ligand fragments originating from copper complexes has also been reported [10,11].

2. Experimental details

The basic experimental apparatus is an adaptation of that discussed previously for phosphorescence experiments [12]

* Corresponding author. Fax: +1 414 288 7066.

SSDI 1010-6030(95)04219-9

and MPI spectroscopy [3]. A Questek v-β excimer laser, operated at 1 Hz, was used to pump a Lambda Physik FL3002 dye laser. The dye laser output was frequency-doubled using a BBO crystal housed in an InRad autotracker. The fundamental was separated from the harmonic and blocked. The final UV laser energy, measured by a Molectron J-25 joule meter, was 0.5 mJ per pulse at each excitation wavelength. The laser was focused in the center of a T-shaped glass cell using a 20 cm focal length lens. The ion collection plates used in the REMPI experiments were removed from the cell for the fluorescence measurements.

The dispersed fluorescence spectra were measured at 90° relative to the excitation laser beam. Emission from the volume of the laser focus was imaged onto the slits of a PTI 1/4 monochromator using two lenses. Fluorescence signals were detected using a Hamamatsu model R1104 photomultiplier tube. The phototube signals were integrated using a computer-controlled home-built gated integrator (Evans Electronics boards) operated in boxcar mode. Data acquisition and monochromator scanning were controlled using a Northgate 386 PC. The monochromator was stepped in 0.5 nm increments and 200 laser shots were averaged per wavelength.

Samples of DBTDA (Pfaltz and Bauer, 95%) were prepared by degassing via multiple freeze–pump–thaw cycles in liquid nitrogen. The only detectable contaminant was a larger, less volatile, complex consistent with a dimeric di-tin hydrolysis product [3] which is not expected to interfere with the experiments performed here. The gas-phase absorption spectrum of DBTDA was measured at its room-temperature vapor pressure, in 1 atm of air, with a Perkin-Elmer 320 spectrophotometer.

Fluorescence experiments were performed on room-temperature, continuously flowing, 50 mTorr samples of DBTDA. Sample pressures were monitored using a Baratron capacitance manometer. The front window of the reaction cell was rotated after approximately 2×10^6 laser shots in order to minimize the effects of photoproduct deposition on the CaF_2 window.

3. Results

The gas-phase absorption spectrum of DBTDA is shown in Fig. 1. The onset of absorption at approximately 240 nm is similar to that observed for the $^1(n,\pi^*)$ chromophore in organic esters [13]. The one-photon wavelengths used for the MPD/LIF experiments are also indicated in Fig. 1.

A broad structure, not consistent with atomic transitions, was observed [3] in the DBTDA total ion current MPI spectrum at one-photon energies of 42 250–42 500 cm^{-1}. Excitation at 236.28 nm was chosen as representative of this region for the MPD/LIF experiments. This wavelength corresponds to a position between two REMPI peaks. Fig. 2 shows typical results for a 50 mTorr sample of DBTDA. Weak emission was observed with one band centered at 390

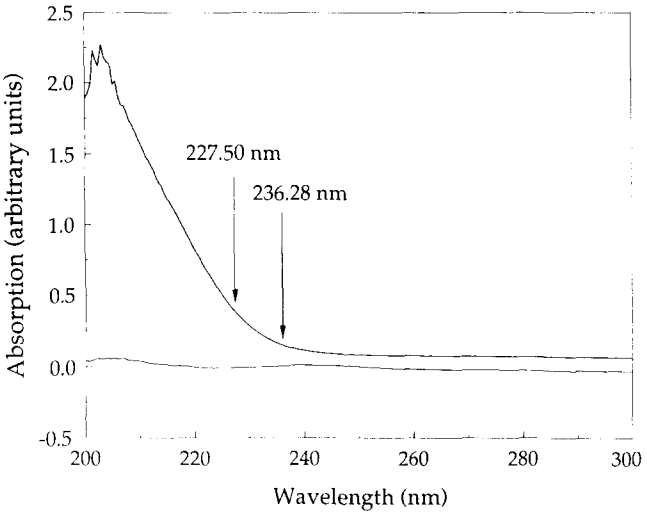

Fig. 1. UV absorption spectrum of DBTDA. The spectrum was obtained with 2 nm resolution. No absorption was observed at wavelengths above 300 nm. The top trace is the DBTDA spectrum and the bottom trace was obtained with an empty cell.

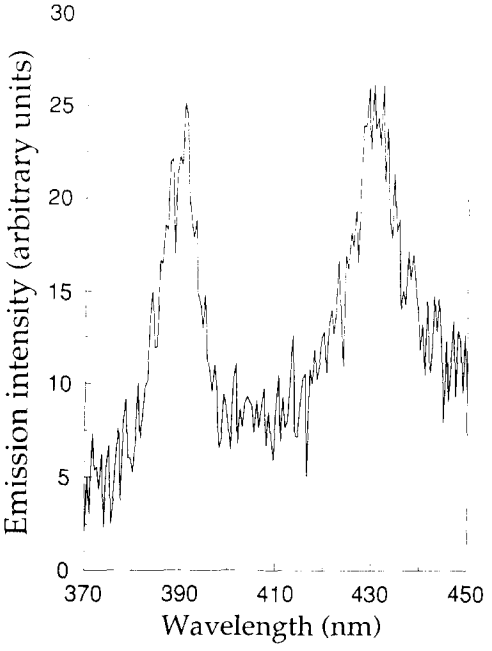

Fig. 2. Dispersed emission spectrum. The one-photon excitation wavelength was 236.28 nm. Other experimental conditions are given in the text.

nm and a second band observed at 430 nm. Emission signals were weak and no observable wavelength dependence on the MPD/LIF spectrum was found with one-photon excitation energies in the range 42 250–42 500 cm^{-1}.

In order to obtain larger LIF signals, the excitation wavelength was shifted to 227.5 nm. This provides a better one-photon initial absorption by DBTDA, as indicated in Fig. 1, at a wavelength where good UV powers can still be generated in our apparatus. The resulting MPD/LIF spectrum for a 50 mTorr DBTDA sample is shown in Fig. 3. The two bands observed in Fig. 2 are also found at this excitation wavelength, although the intensity of the 430 nm band is increased relative

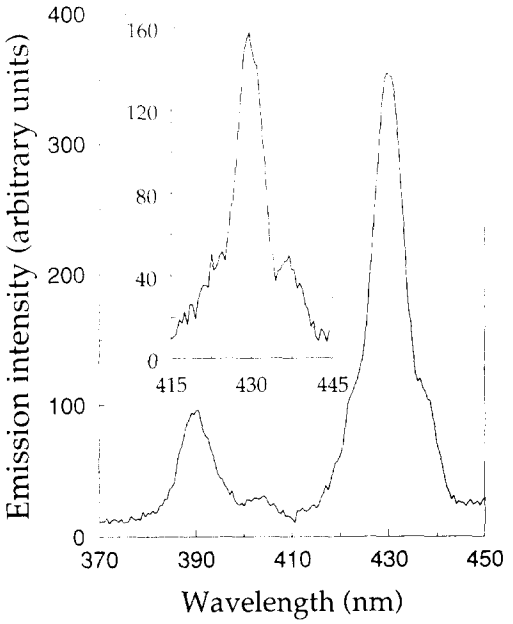

Fig. 3. Dispersed emission spectrum. The one-photon excitation wavelength was 227.5 nm. Other experimental conditions are given in the text. The inset shows the 430 nm band at slightly higher resolution.

to the 390 nm band. In addition, a weak band is observed at approximately 403 nm. The intense 430 nm band appears to have shoulders on each side and a scan performed at the limit of the monochromator resolution is shown in the inset of Fig. 3.

4. Discussion

The LIF spectra shown in Figs. 2 and 3 are not consistent with the known Sn transitions [14], eliminating the atomic product as the source of the emission. A second potential Sn-containing fragment, SnO, was considered since the unidentified structure in the REMPI spectrum was observed in the region of the one-photon $E \leftarrow X$ transition [15]. Emission from several excited states of SnO has been observed in the 300–600 nm range [16–18]. No emission was observed in our experiments at wavelengths above 450 nm where the intense SnO ($a^3\Sigma^+(1)$–$X^1\Sigma^+$) system is reported [15–17]. The feature at 390 nm in Figs. 2 and 3 is also inconsistent with the expected SnO bands.

Another possible source of the observed REMPI structure is the Rydberg transitions of CH [19]. The features at 390 nm and 430 nm coincide exactly with the CH ($B^2\Sigma^-$–$X^2\Pi$) and ($A^2\Delta$–$X^2\Pi$) 0–0 bands respectively [19]. The contour of the $A \rightarrow X$ band shown in the inset of Fig. 3 is similar to that observed in higher resolution measurements of CH excited via LIF in atmospheric pressure flames [20] and generated via electron-impact dissociation of methyl halides [21]. Nearly identical spectral resolution of this CH band has been reported for laser photolysis fragmentation-fluorescence spectrometry (LPF-FS) experiments on CH_3NO_2 at 193 nm [10]. While the 0–0, 1–1 and 2–2 bands of the CH $A \rightarrow X$ transition overlap [21], the 1–1 band of the $B \rightarrow X$ transition, observed at approximately 403 nm [22], should be resolvable in our apparatus. A weak band at this wavelength is evident in Fig. 3.

The results obtained here are analogous to the observation of ligand-derived CH generated from UV MPD of bis(1,1,1-trifluoroacetylacetonato)copper(II) [10] and Cu(II), Al(III), Fe(III), Cr(III) and Ga(III) with 1,1,1,5,5,5-hexafluoro-2,4-pentanedione ligands [11]. Fluorescence from metal atoms was also observed in these experiments, as well as emission from the Fe(III) complex at 389.3 nm which was assigned to the CO ($C^1\Sigma^+$–$A^1\Pi$) 0–1 Herzberg band [10,11]. Our spectral resolution would not be sufficient to discriminate between the CO $C \rightarrow A$ 0–1 and the CH $B \rightarrow X$ 0–0 transitions. Two factors lead us to reject CO as the source of our 390 nm band. First, no evidence was obtained in our spectra for the CO $C \rightarrow A$ 0–2 transition at 412.5 nm, which has a slightly larger Franck–Condon factor than the 0–1 band [22]. The second piece of supporting evidence for CH B–X emission is the observation of a peak consistent with the CH $B \rightarrow X$ 0–1 transition.

The source of CH fragments in the UV MPD of DBTDA may be either the *n*-butyl or the acetate ligand. Based on the photochemistry of organic esters [13], excitation of the $^1(n,\pi^*)$ chromophore, which is localized on the carbonyl group, should result in Norrish type I α-cleavage or Norrish type II molecular elimination. Loss of CH_3 from the acetate ligand via a Norrish type I channel, followed by thermal decarboxylation, is a likely source of the small yield of CO_2 observed in one-photon experiments [3]. CH_3 is a source of CH, as shown in LPF-FS experiments on nitromethane at 193 nm [10]. Dissociation of CH_3 via two single-photon absorption steps, each followed by the loss of one H atom, or two-photon excitation followed by dissociation into CH and H_2 have been proposed as possible mechanisms [10]. In addition, UV MPD/LIF experiments performed on small organic species, such as CH_2CO, have resulted in the detection of CH [23]. Additional investigations are required to characterize the ligand fragmentation mechanism and to clarify whether CH is the source of the structure in the REMPI spectrum of DBTDA.

5. Conclusions

UV MPD of di-*n*-butyl tin diacetate results in extensive ligand fragmentation in addition to atomic Sn formation. Emission from the CH ($B^2\Sigma^-$–$X^2\Pi$) 0–0 and 0–1 bands and the ($A^2\Delta$–$X^2\Pi$) band is observed via one-color MPD/LIF spectroscopy.

References

[1] A. Gedanken and M.B. Robin, *J. Phys. Chem.*, *86* (1982) 4096.
[2] D.A. Gobeli, J.J. Yang and M.A. El-Sayed, *Chem. Rev.*, *86* (1985) 529.

[3] J.M. Hossenlopp, T.R. Viegut and J.A. Mueller, in J. Chaiken (ed.), *Laser Chemistry of Organometallics,* ACS Symposium Series 530, 1993, p. 75.
[4] J.M. Hossenlopp, K.A. Storne and J. Chaiken, *J. Phys. Chem., 96* (1992) 2994.
[5] Z. Karny, R. Naaman and R.N. Zare, *Chem. Phys. Lett., 59* (1978) 33.
[6] D.P. Gerrity, L.J. Rothberg and V. Vaida, *J. Phys. Chem., 87* (1983) 2222.
[7] G.W. Tyndall, C.E. Larson and R.L. Jackson, *J. Phys. Chem., 93* (1989) 5508.
[8] S.A. Mitchell and P.A. Hackett, *J. Chem. Phys., 93* (1990) 7813.
[9] D.P. Gerrity and S. Funk, in J. Chaiken (ed.), *Laser Chemistry of Organometallics,* ACS Symposium Series 530, 1993, p. 26.
[10] E.L. Wehry, R. Hohmann, J.K. Gates, L.F. Guilbault, P.M. Johnson, J.S. Schendel and D.A. Radspinner, *Appl. Opt., 26* (1987) 3559.
[11] J. Schendel and E.L. Wehry, *Anal. Chem., 60* (1988) 1759.
[12] T.R. Viegut, P.J. Pisano, J.A. Mueller, M.J. Kenney and J.M. Hossenlopp, *Chem. Phys. Lett., 195* (1992) 568.
[13] J.G. Calvert and J.N. Pitts, Jr., *Photochemistry,* Wiley, New York, 1966, Chapter 5.
[14] C.E. Moore, Atomic energy levels, *Natl. Stand. Ref. Data Ser., (U.S.) Natl. Bur. Stand., 3* (1971).
[15] S.N. Suchard (ed.), *Spectroscopic Data,* Vol. 1, Part B, Plenum, New York, 1975, p. 1061.
[16] W. Felder and A. Fontijn, *Chem. Phys. Lett., 34* (1975) 398.
[17] G.A. Capelle and C. Linton, *J. Chem. Phys., 65* (1976) 5361.
[18] M.A.A. Clyne and M.C. Heaven, *J. Chem. Soc., Faraday Discuss., 71* (1891) 213.
[19] K.P. Huber and G. Herzberg, *Molecular Spectra and Molecular Structure,* Vol. 4, Van Nostrand Reinhold, New York, 1979.
[20] N.L. Garland and D.R. Crosley, *Appl. Opt., 24* (1985) 4229.
[21] Y. Ito, A. Fujimaki, K. Kobayashi and I. Tokue, *Chem. Phys., 105* (1986) 417.
[22] K. Mikulecky and K.-H. Gericke, *J. Chem. Phys., 98* (1993) 1244.
[23] P.H. Krupenie, The band spectrum of carbon monoxide, *Natl. Stand. Ref. Data Ser., (U.S.) Natl. Bur. Stand., 5* (1966).
[24] B.B. Craig, W.L. Faust and S.K. Chattopadhyay, *J. Chem. Phys., 85* (1986) 4995.